Received: 3 April 2019 | Revised: 5 June 2019 | Accepted: 7 June 2019
DOI: 10.1002/qua.26009

FULL PAPER

International Journal of QUANTUM CHEMISTRY WILEY

Theoretical and experimental investigation of geometry and stability of small potassium-iodide K_nI (n = 2–6) clusters

Branislav Milovanović[1] | Milan Milovanović[1] | Suzana Veličković[2] | Filip Veljković[2] | Aleksandra Perić-Grujić[3] | Stanka Jerosimić[1]

[1]Faculty of Physical Chemistry, University of Belgrade, Belgrade, Republic of Serbia
[2]University of Belgrade, Vinča Institute of Nuclear Sciences, Belgrade, Republic of Serbia
[3]Faculty of Technology and Metallurgy, University of Belgrade, Belgrade, Republic of Serbia

Correspondence
Milan Milovanović, Faculty of Physical Chemistry, University of Belgrade, Studentski trg 12-16, P.O. Box 47, PAC 105305, 11158 Belgrade, Republic of Serbia.
Email: milanm@ffh.bg.ac.rs

Funding information
Ministry of Education, Science, and Technological Development of the Republic of Serbia, Grant/Award Numbers: ON-172019, ON-172040

Abstract

Small heterogeneous potassium-iodide clusters are investigated by means of ab initio electronic structural methods together with experimental production and detection in mass spectrometry. Experiments were done by using Knudsen cell mass spectrometry (KCMS) modification method, which provided simultaneous generating of all $K_nI^{0,+1}$ (n = 2–6) clusters at once. Clusters with more than two potassium atoms are produced for the first time. The lowest lying isomers of those $K_nI^{0,+1}$ (n = 2–6) clusters were found by using a random-kick procedure. The best description of growth of these clusters is the addition of one potassium atom to a smaller-neighbor cluster. Subsequently, stability of these species was examined. In spite of general trend of decreasing of binding energies, the closed-shell species have slightly larger stability with respect to the open-shell species. Alternation of dissociation energies between closed-shell and open-shell clusters is presented. Experimental setup also allows determination of ionization energies of clusters: the obtained values are in the range of 3.46–3.98 eV, which classify these clusters as "superalkali." For closed-shell clusters, the theoretical adiabatic ionization energies are close to experimental values, whereas in the case of open-shell clusters, the vertical ionization energies are those that are close to experimental values.

KEYWORDS
B3P86, potassium-iodide clusters, RCCSD[T], superalkali, surface ionization mass spectrometer

1 | INTRODUCTION

Clusters are aggregates of a finite number of atoms or molecules, which often display properties that differ both from the individual components and the bulk. Therefore, they are considered as unique state of matter. Clusters play a vital role in the vapor-to-condensed phase transition of all matter. For small cluster sizes, a single atom more or less can make a dramatic difference; in contrast, for large clusters, properties change smoothly with increasing size, which is often connected to the surface/volume ratio. The studies of metal clusters have attracted wide attention both on theoretical and experimental work due to their possible application as building blocks of matter.[1,2] Clusters consisting of an alkali metal combined with a more electronegative element have ability to form stoichiometric, $(MX)_n$, and nonstoichiometric heterogeneous clusters, M_nX_{n-m} (M—alkali metal atom, X—nonmetal, $n > m$).[3–5]

The first theoretical work on the nonstoichiometric clusters of the type M_nX was reported by Schleyer[6] They have shown that the "excess" electron delocalizes over the alkali atoms forming a covalent M-M bond, that is, the alkali "cage." The binding in M_nX clusters ($n \geq 2$) has to be

 © 2019 Wiley Periodicals, Inc.

considered as fundamentally ionic, between positive charged "cage" of alkali atom (M_n^+) and negative charged nonmetal (X^-). Subsequently, Gutsev[7] have reported that clusters, M_nX, exhibit lower ionization energies than alkali metal atoms (5.39–3.89 eV). In contrast, MX_n clusters have been predicted to have very high electron affinity, substantially higher than halogen atoms. Therefore, clusters M_nX and MX_n have been called "superalkalis" and "superhalogens," respectively.[7–9] Very exciting development in the field of clusters is the realization that stable "superalkali" and "superhalogeni" clusters, with suitable size and composition, can be designed to mimic the chemical behavior of atoms in the periodic table. Consequently, they can be described as superatoms, and may serve as potential building block for the new cluster assembled materials with unique structural, electronic, optical, magnetic, and thermodynamic properties.[10,11]

Much theoretical and experimental work was reported on properties of pure potassium cluster species.[12–18] Also, many heterogeneous clusters of potassium, among them potassium iodide clusters, are experimentally and theoretically investigated. The structural and bonding properties of the fully ionic stoichiometric potassium iodide cluster, $(KI)_n$ ranging in size from 2 to 500, were studied theoretically and experimentally.[19–21] The nonstoichiometric potassium iodide clusters of the form $M(MX)_n$ and $(MX)_nX$ were detected by mass spectrometric techniques.[22–24] Metal-rich nanoclusters such as $K_{2-5}(KI)_n^+$ ($n \sim 27$) were produced by a supersonic cooling source combined with a laser ablation source.[22] Furthermore, secondary ion mass spectrometry by ion bombardment of potassium iodide resulted in cluster ions of the form $[K(KI)_n]^+$, $n = 22$.[24] The clusters $I^-(KI)_n$, $K^+(KI)_n$ have been recorded in the mass spectra by using the fast Xe atom bombardment method. It has been found that the mass spectral pattern of $I^-(KI)_n$ cluster ions was similar to that of $K^+(KI)_n$ cluster ions.[23] Furthermore, the nonstoichiometric potassium rich anions, $K(KI)_n^-$ and $K_2(KI)_n^-$, were produced by vaporization of a solid KI sample using laser-vaporization cluster source.[19] Then, in desorption ionization mass spectra the positively charged clusters of the general formula $K_nI_{n-1}^+$ (n = 2 and 3) often occur.[25–27]

Potassium halide adducts of the form K_2X^+, desorbed from neutral salts by high power pulsed infrared laser radiation, were detected by Fourier transform ion cyclotron resonance mass spectrometry (FT-ICR). Among the potassium halides, KI generates the highest ratio of detected K_2I^+ to K^+, therefore it is the best choice for cation-transfer reactions in infrared laser desorption ionization FT-ICR.[26] To complete the survey of previously reported studies, we mention the production of K_2I^+ ions from solution of potassium iodide salt in methanol by electrospray ionization (ESI), which is of importance for protein analysis by ESI mass spectrometry.[26] Additionally, the K_2I^+ ions were formed by the surface ionization mass spectrometry using triple filament technique.[28] Generally speaking, alkali halide clusters have been used as samples for understanding of the electrospray, nanospray and ionspray ionization mechanism.[25,29] To the best of our knowledge, there is no data available in the literature about the formation, stability and the ionization energies of any of the K_nI, $n > 2$ clusters.

In the present study, the structure and stability of small potassium-iodide $K_nI^{[0,+1]}$ (n = 2–6) clusters, using both experiments and theoretical predictions, are under investigation. In Section 2, the details of experimental detection will be presented. The subsequent Section 3 will provide the details of the quantum chemical calculations. In Section 4, we show the experimental and theoretical results with discussion. In the last Section 5, the present conclusions are given.

2 | EXPERIMENTAL DETECTION

The Knudsen cell mass spectrometry (KCMS) proved to be very significant method for formation and characterization of homogeneously and heterogeneously metal clusters.[30,31] Also, previous results have shown that the surface ionization mass spectrometer represents a powerful tool for investigation of "superalkali" clusters of the type M_nX (M—alkali atoms, X—nonmetal). Experimental setup used in this study is home-built setup, which implies the Knudsen cell (KC) combined with surface ionization. The details are described elsewhere.[32] Briefly, the Knudsen tantalum cell (7 mm × 6 mm with an orifice diameter 0.1 mm) is equipped with a tungsten heater positioned at the bottom of this cell. The cell is placed in the ionization chamber of a single focusing magnetic sector mass spectrometer. A sample of KI salt compressed into a ring shape was located next to the KC's inner wall near the lid, at atmospheric pressure. Temperatures of the KC and the tungsten heater were controlled separately. In our experimental setup, the tungsten heater was controlled in the temperature range between 500 and 2700 K. The tungsten heater was used for ionization. Identification of each cluster ion formed by this experimental setup was determined according to its mass-to-charge ratio and natural isotopic abundances of elements potassium (93.26% ^{39}K, 0.01% ^{40}K, and 6.73% ^{41}K) and iodine (100% ^{127}I).

The ionization energies of the iodine-doped potassium clusters were obtained by the Saha–Langmuir equation:

$$I_i = A\exp\left(\frac{\Phi - \mathrm{IE}_i}{kT}\right), \tag{1}$$

where I_i—the ion intensity [i are K^+ or K_nI^+]; A—the term containing reflection coefficients and statistical weighting factors; Φ—the work function of the ionization filament; IE_i—the ionization energies of clusters or atoms; k—the Boltzman's constant; T—the temperature of the tungsten heater. The value of Φ depends on the type of ions, which are adsorbed at the tungsten heater. However, by dividing the Saha–Langmuir equation for K^+ and K_nI^+, the work function from Equation (1) is eliminated.

$$\ln \frac{I(K^+)}{I(K_nI^+)} = \frac{IE(K_nI^+) - IE(K^+)}{kT}. \quad (2)$$

Actually, the IEs of potassium iodide clusters were determined by measuring the intensity of potassium ions and the intensities of the most abundant isotopes of K_nI^+ cluster ions vs the temperature of the heater.

3 | COMPUTATIONAL METHODS

The lowest-lying isomers of potassium-iodide K_nI (n = 2–6) clusters were found by using a random-kick procedure, which represents a variant of the stochastic search method, first reported by Saunders,[33] and later modified by Tai and Nguyen.[34] This randomized algorithm was already used for obtaining the lowest isomers of heterogeneous lithium clusters, Li_nI[35] (n = 2–6) and Li_nCl_m[36] ($n > m$, n = 1–6, m = 1–3). It consists of two parts. The first part is to randomly kick each atom of an initial structure, given by Cartesian coordinates (x_i, y_i, z_i) within the sphere of a radius R to define new atom's set of coordinates($x_i + dx_i$, $y_i + dy_i$, $z_i + dz_i$), where both minimum and maximum distances between two atoms in the structure can be controlled. The second part is to pass the obtained structure to electronic structure software, for a geometry optimization. For an initial structure, we used a structure with all atoms at the origin. As we expected, to get many nuclear configurations with large radius, as in the case of lithium-iodide Li_nI (n = 2–6) clusters, we did not specify maximum distance between atoms, but the kicking procedure was done within spheres of radii $R = 1.0 - 6.5$ Å and with different minimum distances of $D_{min} = 1.0 - 3.0$ Å. The obtained species were then submitted to geometry optimization and frequency calculations by using density functional theory (DFT), specifically B3P86 functional[37,38] with the small 3-21G atomic basis set.

Using simplifying assumptions that probability of finding any particular isomer is the same as for all the others, the approximate probability of finding an isomer is about 95% if one takes three kicks for every minimum to be found.[33] This probability rises to 99.3% (99.9%) if one takes five (seven) kicks for each minimum. Of course, number of isomers is not known initially; but the rate of appearance of new minima decreases as kicking procedure proceeds, and one gets a good idea about the total number that might be found. Using this estimation, we did at least five times as many kicks as there were found minima for all species, with the addition of linear structures (which is rarely obtained with above mentioned initial structure), in order to explore a sufficient number of low-lying energy isomers and find the lowest energy (LE) isomer.

The previously obtained molecular structures were further refined by using the same B3P86 functional, with small core scalar relativistic energy-consistent pseudopotentials and correlation consistent basis sets. For potassium, the pseudopotential includes 10 core electrons, and basis set consists of [8s 8p 5d 3f] contractions [this combination is further denoted as ECP10MDF][39]; for iodide, the pseudopotential includes 28 core electrons and basis set consists of [5s 4p 3d 1f] contractions [further denoted as cc-pVTZ-PP].[40] At the same level of theory, we have calculated the zero-point vibrational energy (ZPVE) corrections.

In order to analyze the impact of basis sets on the structural parameters, geometry optimizations of KI and KI^+ with a series of correlation consistent basis sets were performed. In the case of K atom, we used the already mentioned ECP10MDF. For iodine atom, together with the pseudopotential, triple- and quadruple-zeta [(aug-)cc-pVXZ-PP, X = T, Q] basis sets were used,[40] and additionally the weighted core-valence correlation consistent triple- and quadruple-zeta (cc-pwCVXZ-PP, X = T, Q) basis sets.[41] Also, we have investigated changes due to using different functionals: B3LYP,[37,42] B3P86, and B3PW91[37,43]; additionally, the coupled cluster method was used, with correlation of all electrons denoted as RCCSD[T]—which is short from the restricted open-shell singles and doubles coupled-cluster, with restricted Hartree–Fock wave function as a reference, with perturbative inclusion of triples.[44–46]

In Supporting Information Table S1, we show equilibrium bond distances of KI and KI^+ calculated at different levels of theory mentioned above. The only available experimental equilibrium bond length is (3.0478 ± 0.0004) Å for KI.[47] This experimental value is almost perfectly predicted with both B3P86 and RCCSD(T) using ECP10MDF basis set for potassium and cc-pVTZ-PP basis set for the iodine atom (both values are 3.0480 Å). Changing of basis sets from triple- to quadruple-zeta, produce elongation of bond lengths for KI, except for aug-cc-pVXZ-PP basis sets, where the change is very small (at RCCSD(T) level bond length is 0.0015 Å shorter with aug-cc-pVQZ-PP basis). The larger difference is predicted by RCCSD(T) method (~0.007 Å) than by using DFT methods (~0.003 Å). On the contrary, for KI^+ molecule changes from triple- to quadrupole-zeta basis set give shorter bonds [except for RCCSD(T)/ECP10MDF(K), cc-pwCVXZ-PP(I) level]. Furthermore, the augmentation of the basis functions with diffuse functions for both neutral and cation species slightly increased the bond lengths. The effect of inclusion of core functions is found to be similar to the effect of augmentation with diffuse functions.

In conclusion, the best-balanced basis sets for description of geometry of these species are ECP10MDF for K and cc-pVTZ-PP for I atom. Therefore, we have used this basis in combination with the less time-consuming [in respect to RCCSD(T)] DFT method, employing the B3P86 functional, for optimizing geometries of all $K_nI^{0,+1}$ (n = 2–6) clusters. This method is denoted as B3P86/ECP10MDF(K), cc-pVTZ-PP(I). To justify the choice of method for obtaining geometries of larger clusters, we performed high-quality RCCSD(T)/ECP10MDF(K), cc-pVTZ-PP(I) geometry optimization for most stable $K_nI^{0,+1}$ (n = 1–3) clusters and compared them to DFT results in Supporting Information Table S3. As mentioned above,

KI geometries are the same for both methods, while KI^+ bond length obtained with DFT is ~0.04 Å longer than with RCCSD(T). For the most stable K_2I isomer, the RCCSD(T) bond length is shorter for 0.018 Å and angle is 0.2° larger than at the DFT level. Furthermore, for the most stable linear K_2I^+, the difference in bond length is only 0.004 Å for two levels of theory. In the case of the most stable K_3I isomer, K—I bond length is by 0.021 Å shorter, K—K bond is by 0.005 Å longer, whereas K—I—K angle is 0.5° smaller with RCCSD(T) than calculated with DFT method. Again differences are reduced for cation, the bond lengths are by 0.007 Å and 0.005 Å shorter, and angle is 0.3° smaller with RCCSD(T) in respect to DFT method.

Regarding frequencies, harmonic frequencies and ZPVE values of KI and KI^+ calculated at different levels of theory are presented also in Supporting Information Table S2. The only experimental value is of 186.53 cm^{-1} for KI.[48] The time-consuming RCCSD(T)/ECP10MDF(K), cc-pwCVQZ-PP(I) value of 187 cm^{-1} agrees perfectly with the reported experimental value, whereas DFT values are somewhat smaller by 7, 4, and 8 cm^{-1} calculated with B3LYP, B3P86, and B3PW91 functional, respectively. Again, the best agreement with experimental value for DFT method is obtained with B3P86/ECP10MDF(K), cc-pVTZ-PP(I) level of theory (185 cm^{-1}). ZPVE DFT values are ~0.04 kJ/mol lower than corresponding RCCSD(T) values.

In order to calculate the binding, dissociation and ionization energies of the clusters, the single-point RCCSD(T)/ECP10MDF(K), cc-pVQZ-PP(I) calculations were performed at the optimized geometries, for the most stable isomers. As will be shown in subsection 4.4, the values of these properties for $K_nI^{0,+1}$ (n = 1–3) species are not changed when single point calculations were performed at the B3P86/ECP10MDF(K), cc-pVTZ-PP(I) [further denoted as RCCSD(T)/QZ//B3P86/TZ level] or RCCSD(T)/ECP10MDF(K), cc-pVTZ-PP(I) [further denoted as RCCSD(T)/QZ//RCCSD(T)/TZ level] optimized geometries. Thus, for all $K_nI^{0,+1}$ (n = 2–6) clusters the binding, dissociation and ionization energies are calculated at RCCSD(T)/ECP10MDF(K), cc-pVQZ-PP(I) level for B3P86/ECP10MDF(K), cc-pVTZ-PP(I) geometries and ZPVE corrections. This level would be suitable for predicting properties of larger clusters (n > 6) because it is accurate and it is not computationally demanding as RCCSD(T) optimizations.

All DFT computations and geometry optimizations at the RCCSD(T) level were carried out by using Gaussian(R) 09[49] program package. Geometry optimizations at the B3P86 level employed an energy-represented direct inversion in the iterative subspace algorithm (GEDIIS)[50] with quadratically convergent SCF procedure[51] and UltraFine pruned (99590) grid. For harmonic vibrational frequencies and normal modes, the Hessians have been computed analytically. At the end, the single-point coupled cluster calculations were done by using Molpro program package,[52,53] with default convergence criteria.

4 | RESULTS AND DISCUSSION

4.1 | Experimental results

In this work, a series of iodine-doped potassium clusters were detected experimentally for the first time by using the KCMS method combined with the surface ionization. In Figure 1, a typical mass spectrum of the positive charged clusters of the type K_nI^+ (n = 2–6) is presented, obtained by evaporating only KI salt at the temperature heater of 1450 K.

In the mass spectrum, it has been revealed that the strong peaks appear periodically in an interval of m/z 39, suggesting the presence of KI units in the clusters. Peaks corresponding to m/z of 205, 244, 283, 322, 361 were attributed to K_2I^+, K_3I^+, K_4I^+, K_5I^+, and K_6I^+, respectively. As the

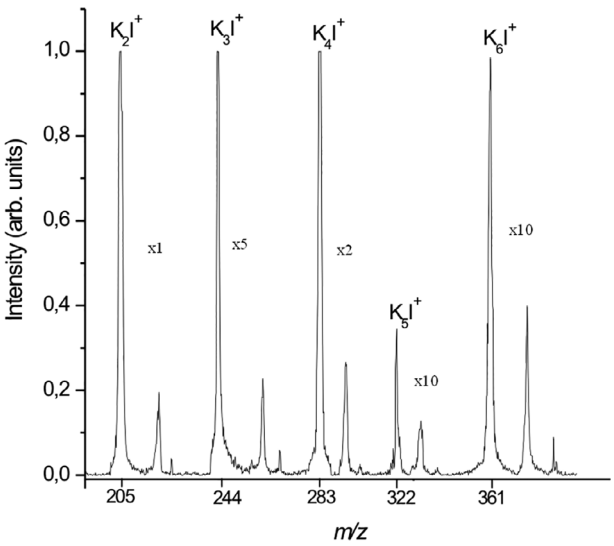

FIGURE 1 The mass spectrum of the positive K_nI^+ (n = 2–6) cluster ions obtained by the evaporation of KI salt at the temperature heater of 1450 K using the modification of KCMS method

heater temperature increase above 1250 K, the first cluster ion that appears in the mass spectrum is K_2I^+. The increasing of the heater's temperature above 1350 K leads to the sharp appearance of all peaks constituting the mass spectrum of KI, including K_3I^+, K_4I^+, K_5I^+, and K_6I^+. The intensity of the K_2I^+ were about two and three times higher than the intensities of the K_4I^+ and K_nI^+ (n = 3 and 6), respectively. Since the intensity of K_5I^+ was four times lower than that of the K_2I^+ ions, it can be concluded that this cluster ions are the most unstable. The experimental setup allow that various cluster ions, such as K_3I^+, K_4I^+, K_5I^+, and K_6I^+, are being formed simultaneously in the same range of temperature (1350–1650 K). It has been also observed that intensities of K_nI^+ ions very slowly increase with the rise of the temperature of heater. At T > 1650 K, the K_nI^+ cluster ions exhibits decomposition and their peaks disappear, leaving only the peaks of the K_2I^+. Because the K_2I^+ appear in the longest range of heater temperature (1250–1750 K), and have the highest intensity, it can be concluded that dipotassium positive ions are the most stable in these experimental conditions.

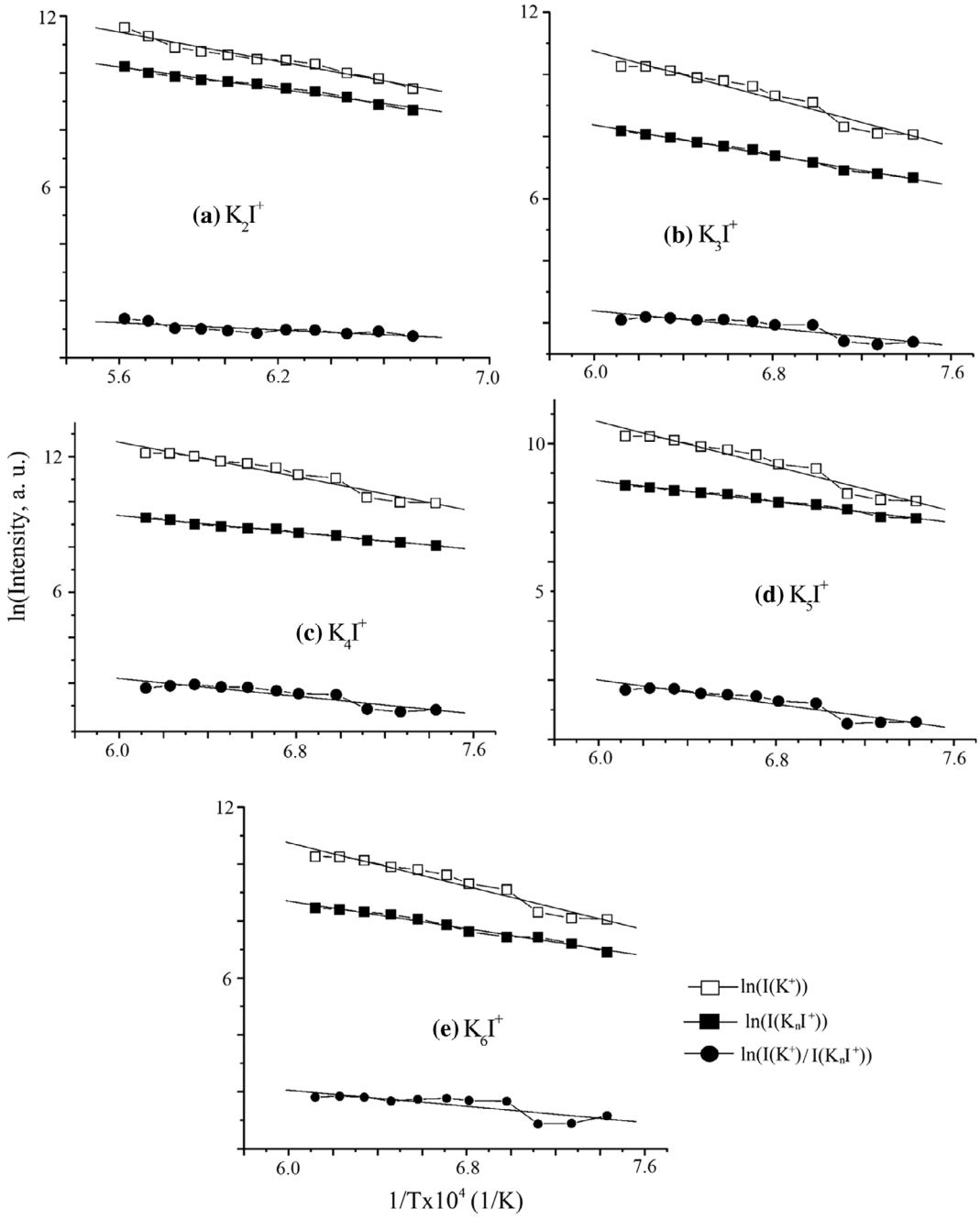

FIGURE 2 Plots of the natural logarithms of positive ion intensities vs 1/T, where T is temperature of the tungsten heater; open square—intensity of K^+ ion; solid square—intensities of K_nI^+ (n = 2–6) cluster ions; solid circle—ln(I[K^+]/I[K_nI^+])

In order to determine the ionization energy of these clusters, the natural logarithms of the ion intensities for K_nI^+ and $^{39}K^+$ as a function of the inverse of heater's temperature (1/*T*) are plotted in Figure 2. For better clarity, the natural logarithms of the ratio of ion intensities for $^{39}K^+$ and K_nI^+ as function of the 1/*T* are represented separately at the same figure. The ionization energies of iodine-doped potassium K_nI (*n* = 2–6) clusters were obtained by using the value of 4.34 eV for the ionization energy of K and the slopes of plots $\ln I(K^+)/I(K_nI^+)$ vs 1/*T* by Equation (2). The obtained ionization energies had the following values: 3.98 ± 0.20 eV for K_2I, 3.74 ± 0.20 eV for K_3I, 3.50 ± 0.20 eV for K_4I, 3.46 ± 0.20 eV for K_5I, and 3.73 ± 0.20 eV for K_6I.

4.2 | Structural isomers of the neutral and cationic $K_nI^{0,+1}$ (*n* = 2–6) clusters

The geometries of all isomers of neutral and cationic clusters up to six potassium atoms ($K_nI^{0,+1}$ [*n* = 2–6]) are displayed in Figures 3–9. Each structure is denoted by the label *x.y.z*, in which *x* stand for the number of potassium atoms, *y* denotes the charge state (*n* for neutral and *c* for cation), and *z* denotes the zth lowest-lying isomer found for that cluster type. Structures which are, based on the geometrical motifs, recognized as the excited states equilibrium geometries of the corresponding *x.y.z* structures, with different spin-multiplicity, are denoted by (*x.y.z*)*. Cluster isomers are furthermore labeled by their empirical formula, with point group symmetry and the ground electronic state (showed in brackets). Relative energies of structural isomers, defined as the single-point energies (with ZPVE correction), calculated at the B3P86/ECP10MDF(K), cc-pVTZ-PP(I) level of theory, of relaxed isomers in respect to the relaxed geometry of the corresponding lowest-lying energy isomer, are shown in Figures 1–7 as well. Because all structures were generated with the random-kick procedure, they were calculated in the framework of the C_1 point group symmetry. However, some of them possess higher symmetry, which was inspected by reoptimization with B3P86/ECP10MDF(K), cc-pVTZ-PP(I) method within

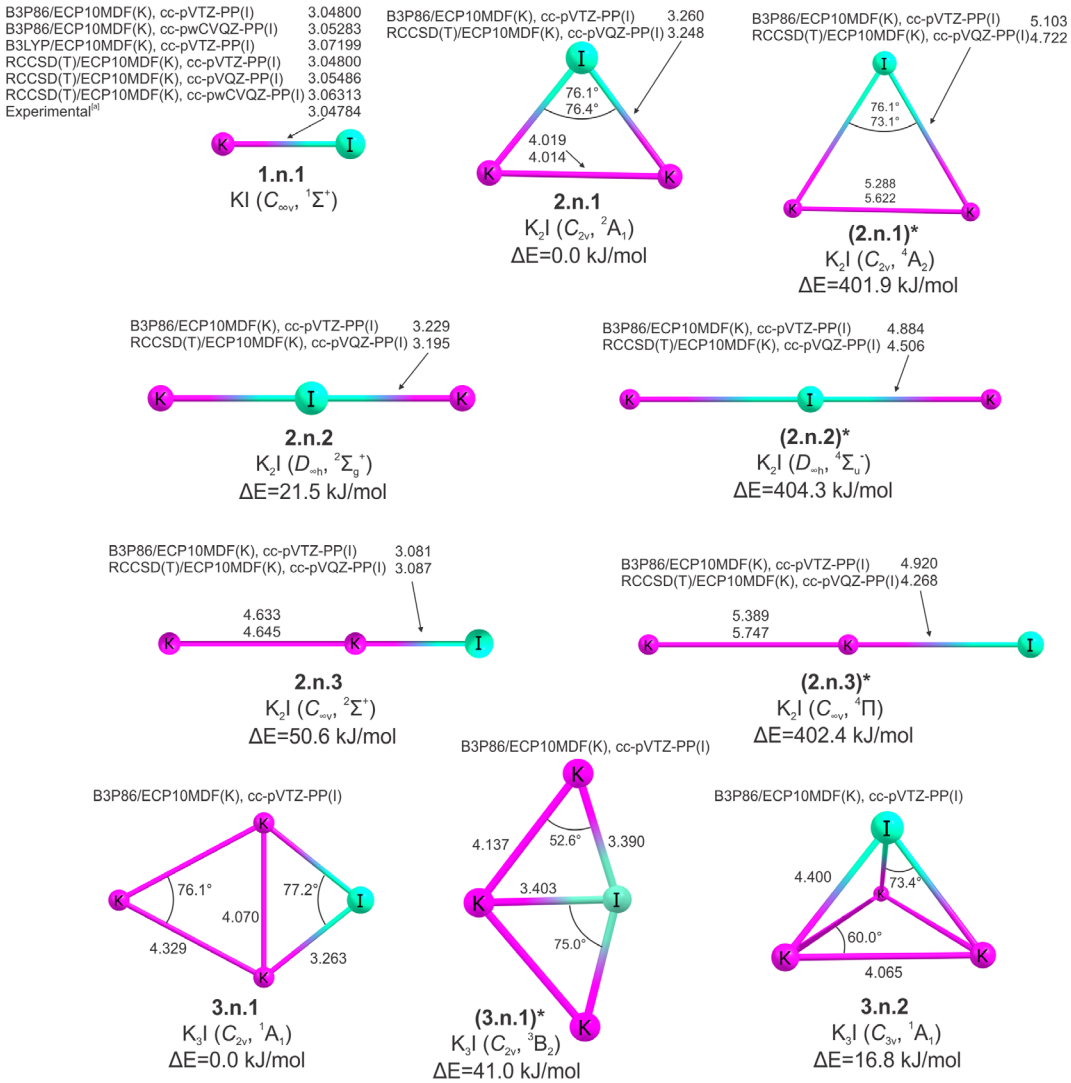

FIGURE 3 Structural isomers of neutral K_nI (*n* = 1–3) clusters. Relative energies (with ZPVE corrections) are calculated with B3P86/ECP10MDF(K), cc-pVTZ-PP(I). Bond distances are given in angstroms and angles in degrees. [a]—Tiemann et al.[47]

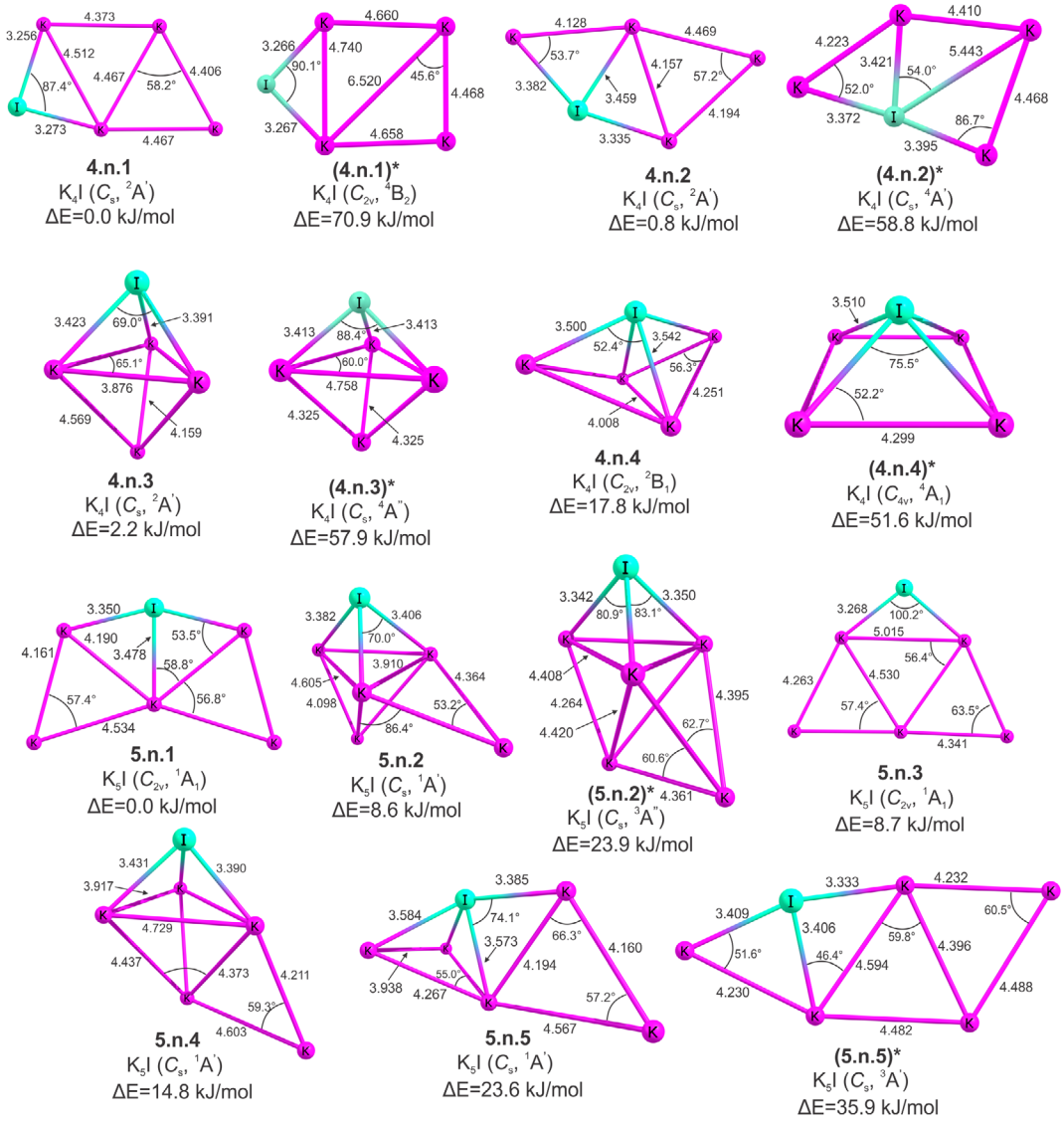

FIGURE 4 Geometries of neutral K_nI (n = 4, 5) clusters. The same type computed data as in Figure 3

the higher symmetry restrictions. In Supporting Information Tables S4 and S5, the relative energies, zero-point vibrational frequencies, and low/imaginary frequencies are presented (in order to distinguish real minima structures and structures that might be transitional) for neutral and cationic species, respectively. It should be noted that structures with vibrational modes, which have frequencies around zero, that is, within the range from 20i cm^{-1} to 20 cm^{-1}, are presented as the structural isomers as well. They could be close to a real minimum because these values strongly depend on numerical accuracy, especially for the flat potential surfaces that are typical for these clusters. Thereby, a few neutral structures: **(2.n.3)***, **(5.n.2)***, **(6.n.1)***, **6.n.6**, and **6.n.11**, possesses low imaginary frequencies in the mentioned range (Supporting Information Table S4); and a handful of cationic structures: **4.c.4**, **4.c.5**, **[4.c.6]***, **5.c.3**, **5.c.4**, **5.c.6**, **6.c.4**, **6.c.5**, **6.c.8**, **6.c.10**, and **(6.c.7)*** also (Supporting Information Table S5).

In Figures 3–9 and in Supporting Information Tables S4 and S5, we present global and local minima structures on the potential energy hypersurfaces. The possibility of having isomers in a higher spin state has also been taken into account by using the random kick procedure described in Section 3. The local minima of higher multiplicity were also presented in Figures 3–9, and these are: **6.n.5**, **6.n.11**, **6.n.12**, **4.c.5**, **4.c.6**, **6.c.6**, **6.c.8**, **6.c.9**, and **6.c.11**. Furthermore, many structures with higher multiplicity were identified, on the basis of their geometrical motifs, as an excited states of the corresponding clusters with lower multiplicity: **(2.n.1)***, **(2.n.2)***, **(2.n.3)***, **(3.n.1)***, **(4.n.1)***, **(4.n.2)***, **(4.n.3)***, **(4.n.4)***, **(5.n.2)***, **(5.n.5)***, **(6.n.1)***, **(6.n.3)***, **(6.n.7)***, **(6.n.10)***, **(2.c.1)***, **(3.c.2)***, **(3.c.3)***, **(4.c.2)***, **(4.c.3)***, **(5.c.1)***, **(5.c.2)***, **[5.c.4]***, **(6.c.5)***, **(6.c.7)***. In addition, two higher spin structures were more stable than the corresponding lower spin clusters: **(4.c.6)** and **(6.c.9)** isomers. Herein, we confirm that the higher spin states structures exist, but typically with relative energy higher than 30 kJ/mol in respect to the relaxed geometry of the corresponding LE isomer, with few exceptions of **(5.n.2)***, **6.n.5**, and **6.c.6** that have relative stabilities of 23.9, 18.1, and 29.1 kJ/mol, respectively.

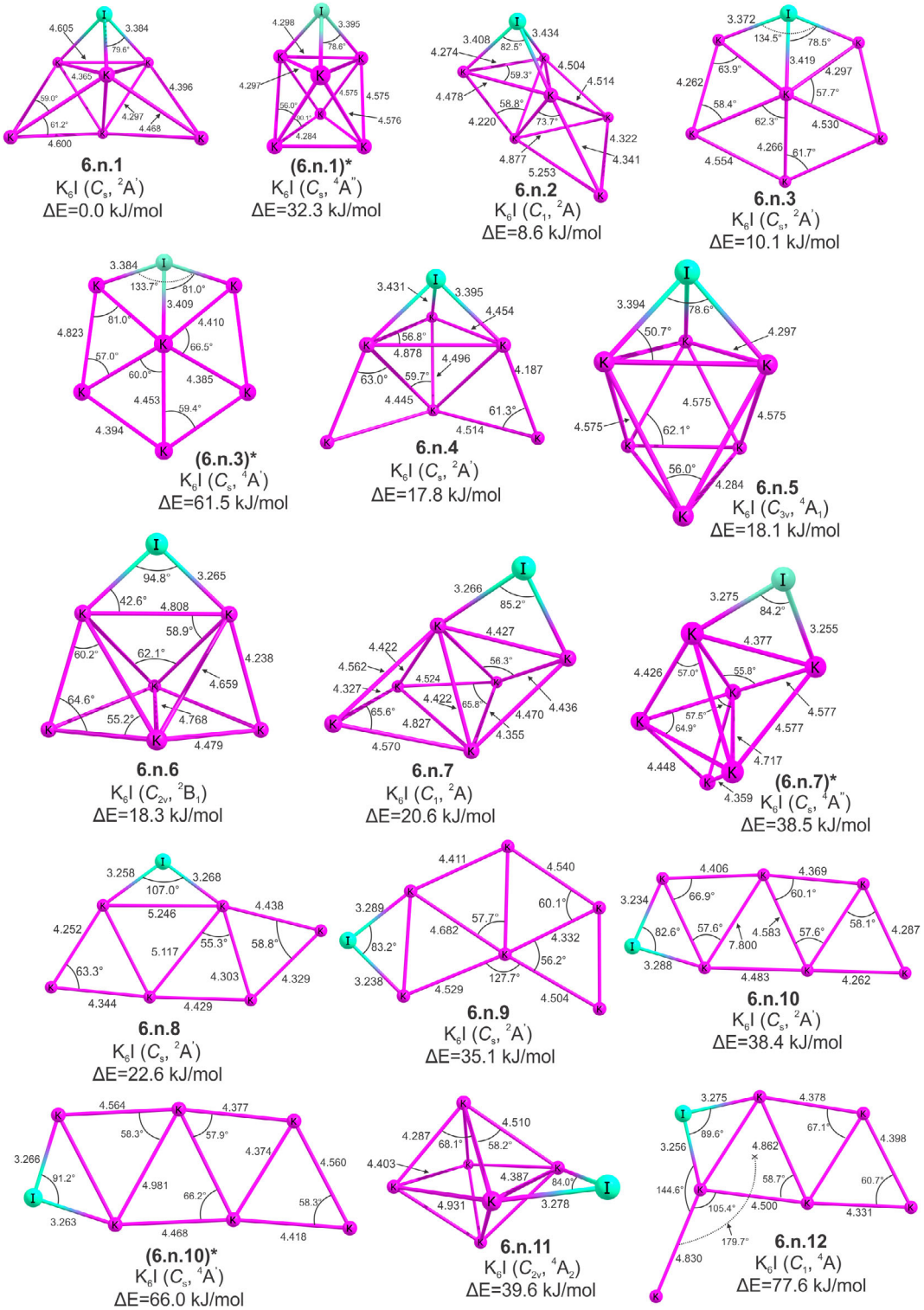

FIGURE 5 Structural isomers of neutral K_nI (n = 6) clusters. The same type computed data as in Figures 3 and 4

Neutral cluster species always have iodine atom located externally (outside of the structure). (Strictly speaking, the iodine atom in linear **2.n.2** and **(2.n.2)*** ($D_{\infty h}$) structures is in between two potassium atoms.) The most stable neutral cluster species up to the n = 5 favor planar structures. We obtained some similar structures to those published for Li_nI (n = 2–6)[35] and Li_nCl (n = 2–6),[36] however, the potential energy surface seems even shallower, and since we included higher spin structures, more isomers are obtained. The change from planar to the 3D most stable structures takes place at six K atom, as in the case of Li clusters. Doublet spin **2.n.2** and **2.n.3** isomers are linear (K—I—K and K—K—I, respectively) and both of them lie above the most stable **2.n.1** isomer with C_{2v} symmetry ($^2A_1$ state). Quartet spin **(2.n.1)***, **(2.n.2)***, and **(2.n.3)*** states lie high above the corresponding global minimum (around 400 kJ/mol). There are in total three K_3I equilibrium geometries: the planar **3.n.1** (C_{2v} structure) as the

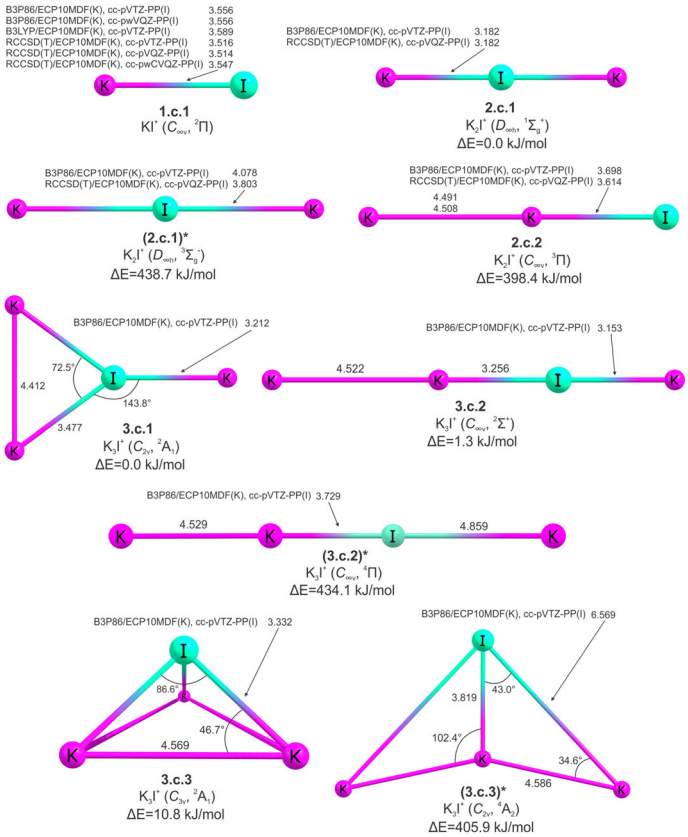

FIGURE 6 Structural isomers of cationic K_nI^+ (n = 1–3) clusters. Relative energies (with ZPVE corrections) are calculated with B3P86/ECP10MDF(K), cc-pVTZ-PP(I). Bond distances are given in angstroms and angles in degrees

most stable one, the **3.n.2** (C_{3v} structure) which is 16.8 kJ/mol above, and the triplet **(3.n.1)*** C_{2v} structure which can be considered as an excited triplet equivalent of the **3.n.1** that lies 41.0 kJ/mol above. Half of (four out of eight) K_4I equilibrium geometries are planar and the most stable is planar as well. Isomers **4.n.1** and **4.n.2** are almost degenerate and **(4.n.3)*** is an excited quartet state of the **4.n.3**. Three out of seven K_5I species isomers are planar, and the most stable is planar again. **5.n.2** and **5.n.3** are almost degenerate and **(5.n.2)*** is an excited triplet correspondent of the **5.n.2**. The most numerous (17 in total) K_6I isomers species are predominantly the 3D structures.

Contrary to the neutral clusters, in many cationic structures, the iodine atom occupies an internal position. In the case of the K_2I^+ and K_3I^+, the lowest-energy isomers are planar, while all other lowest lying isomers have 3D open structures. Number of isomers is 3, 6, 9, 10, and 13 going from K_2I^+ to K_6I^+. After ionization, the geometries of the resulting cationic clusters are significantly distorted as compared to their corresponding neutral species, except for **3.n.2** → **3.c.3**, **4.n.3** → **4.c.1**, **4.n.4** → **4.c.4**, **5.n.1** → **5.c.4**, **5.n.2** → **5.c.1**, and **5.n.4** → **5.c.3**.

4.3 | Growth mechanism

Only in view of geometrical motifs presented in Figures 3–9, the formation of all neutral and charged ($K_nI^{(0,+1)}$, n = 1–6) clusters could be described in one (or more) of the following ways: (a) $K_nI^{(0,+1)}$ formation from $K_{n-1}I^{(0,+1)}$ by adding one potassium atom; (b) $K_nI^{(0,+1)}$ formation from pure $K_n^{(0,+1)}$ by adding iodine atom; (c) $K_nI^{(0,+1)}$ clusters can be considered as a distorted version of pure potassium clusters with the same total number of atoms, $K_{n+1}^{(0,+1)}$.

The first way can be applied on all neutral and cationic potassium-iodide clusters. This growth mechanism is schematically displayed in Figure 10 (LE stands for the lowest energy isomer). Both neutral and cationic cluster species possess two types of structures: 2D planar and 3D structures which can be 3D open (only in cationic case) and 3D compact structures. For neutral clusters, all LE structures up to six atoms are planar, while for cationic ones, the turning point from planar to 3D structures occurs at five atoms. Planar structures are more often present in neutral species. Few cation species, particularly **4.c.6** triplet (or **(4.c.6)*** excited singlet equivalent), **(3.c.3)*** and **4.c.4**, show tendency to grow by two atoms at once and that to **6.c.2**, **5.c.4** doublet (or **(5.c.4)*** excited quartet state) and **6.c.5** structures, respectively, since there is no intermediary structures obtained by the random kick method.

To apply the second or the third way to interpret the cluster growth mechanism, it is necessary to calculate pure potassium clusters structures at the same level of theory as the heterogeneous ones. Anyway, we can find some structural similarities with previously reported structures of pure potassium clusters.[14,17] Finally, we came to the same conclusion as it was for lithium-iodide clusters[35]—the best way to describe the growth of these heterogeneous clusters is by adding one (or two, in special cases mentioned above) potassium atom to $K_{n-1}I^{(0,+1)}$ to obtain $K_nI^{(0,+1)}$ clusters.

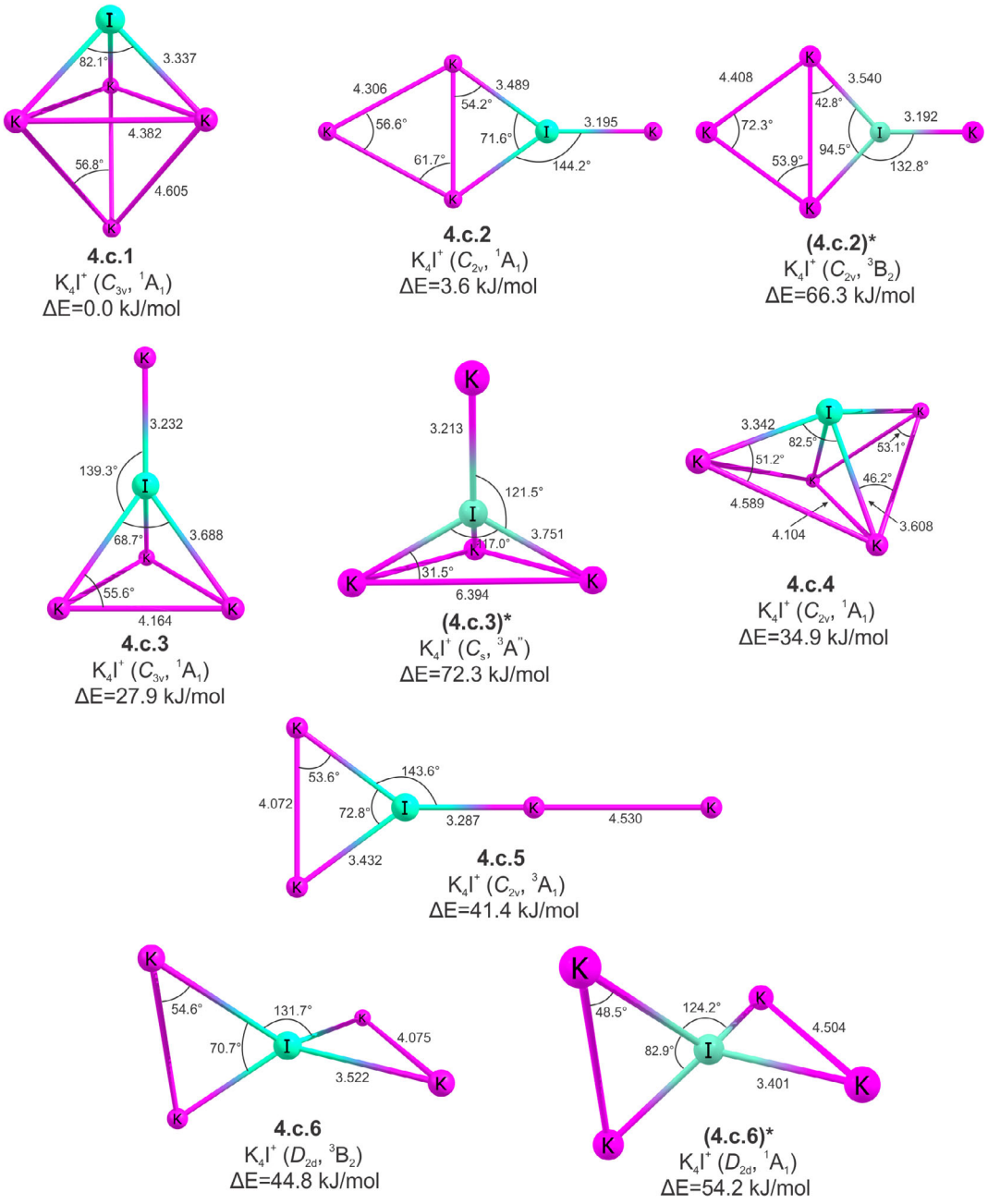

FIGURE 7 Geometries of cationic K_nI^+ (n = 4) clusters. The same type computed data as in Figure 6

4.4 | Stability of neutral and cationic $K_nI^{(0,+1)}$ clusters

4.4.1 | Binding energy per atom

Binding energies (BEs) per atom were calculated for the most stable potassium-iodide $K_nI^{0,+1}$ (n = 2–6) clusters. These values are defined as (with ZPVE corrections included):

$$E_b(K_nI) = \frac{nE(K) + E(I) - E(K_nI)}{n+1}$$
$$E_b(K_nI^+) = \frac{(n-1)E(K) + E(K^+) + E(I) - E(K_nI)^+)}{n+1}.$$

BEs per atom, calculated at two levels of theory: B3P86/ECP10MDF(K), cc-pVTZ-PP(I), and RCCSD(T)/QZ//B3P86/TZ level are presented in Table 1. For $K_nI^{0,+1}$ (n = 1–3) clusters, the RCCSD(T)/QZ//RCCSD(T)/TZ results are also presented in Table 1. The results obtained by using the

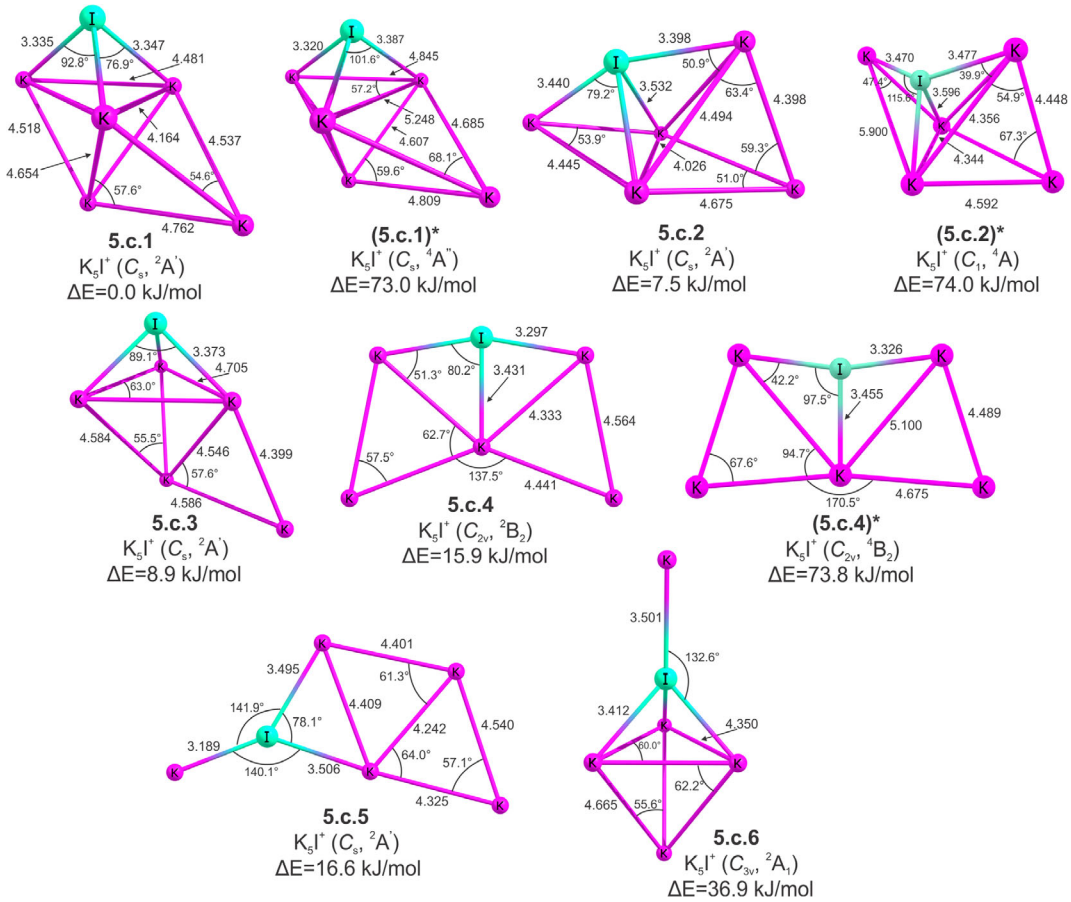

FIGURE 8 Structural isomers of cationic K_nI^+ (n = 5) clusters. The same type computed data as in Figures 6 and 7

first two methods are in good agreement for all clusters (the largest difference is of 0.06 eV), while RCCSD(T)/QZ//B3P86/TZ and RCCSD(T)/QZ//RCCSD(T)/TZ results for $K_nI^{0,+1}$ (n = 1–3) are the same.

Potassium-iodide (KI) and its cation (KI^+) are ionic salts. Species K_2I^+, similar to corresponding lithium-chloride cluster Li_2Cl^+,[36] is recognized as ionic species. Hence, their properties are different from other species discussed here. One can see distinctively high BE per atom that possess neutral KI (1.78 eV) and cationic K_2I^+ (1.75 eV) species. On the other hand, the electron deficient species KI^+ has very low BE energy (of 0.16 eV).

Considering both neutral and charged clusters, the trend is the decreasing of BE with increasing number of K atoms. Going from K_2I to K_6I, the differences in BE between adjacent clusters are 0.14 eV, 0.19 eV, 0.03 eV, and 0.08 eV. For cationic clusters the differences are 0.08 eV, 0.15 eV, and 0.03 eV going from K_3I^+ to K_6I^+. From these values one can see that, in spite of general trend of decreasing BE, some clusters have slightly increased stability—these are: K_3I, K_5I, K_4I^+, and K_6I^+. These clusters have an even number of electrons—they are closed-shell species; on the contrary, the open-shell species that have an odd number of electrons are relatively less stable: K_2I, K_4I, K_6I, K_3I^+, and K_5I^+. We have already shown by means of the natural bond orbital (NBO) analysis,[35] that in the case of Li_nI clusters, the important reason for higher stability of closed-shell species is the delocalization of the 3center/2electron type, which is more energetically favored than the typical 2center/2electron bonds. Although we have not used the NBO analysis in this work, we can assume that electronic structures of presented potassium iodide clusters are very similar to lithium iodide clusters, and that the reason for higher stability of the closed-shell species is the same.

The calculated BE values of pure potassium K_n (n = 2–7) clusters are: 0.25 eV, 0.23 eV, 0.29 eV, 0.32 eV, 0.37 eV, and 0.37 eV, respectively.[18] Comparing homogeneous and heterogeneous clusters, one can see that doping of potassium clusters with iodide significantly contribute to their stability. However, heterogeneous K_nI clusters are less stable than corresponding Li_nI clusters.[35] Taking into account that the measured binding (cohesive) energy for bulk potassium ($n \rightarrow \infty$) is of 0.94 eV,[54] one can conclude that BE for K_nI clusters decrease to a minimum value for some n and then increase to the bulk limit, where iodide atom could be considered as impurity.

From experimental mass spectrum in Figure 1, it can be seen that K_2I^+ ions appear to be highly stable having the highest peak's intensity; the next is K_4I^+ which has greater intensity than K_3I^+, then K_6I^+, and the cluster ion with the lowest peak's intensity is K_5I^+. Theory predict the highest stability of K_2I^+, but BE value for K_4I^+ is not higher than BE for K_3I^+, and BE for $K_6I^+$is not higher then K_5I^+. Thus, using only this criterion for the stability of clusters, we cannot totally explain the experimentally obtained stability of the cations.

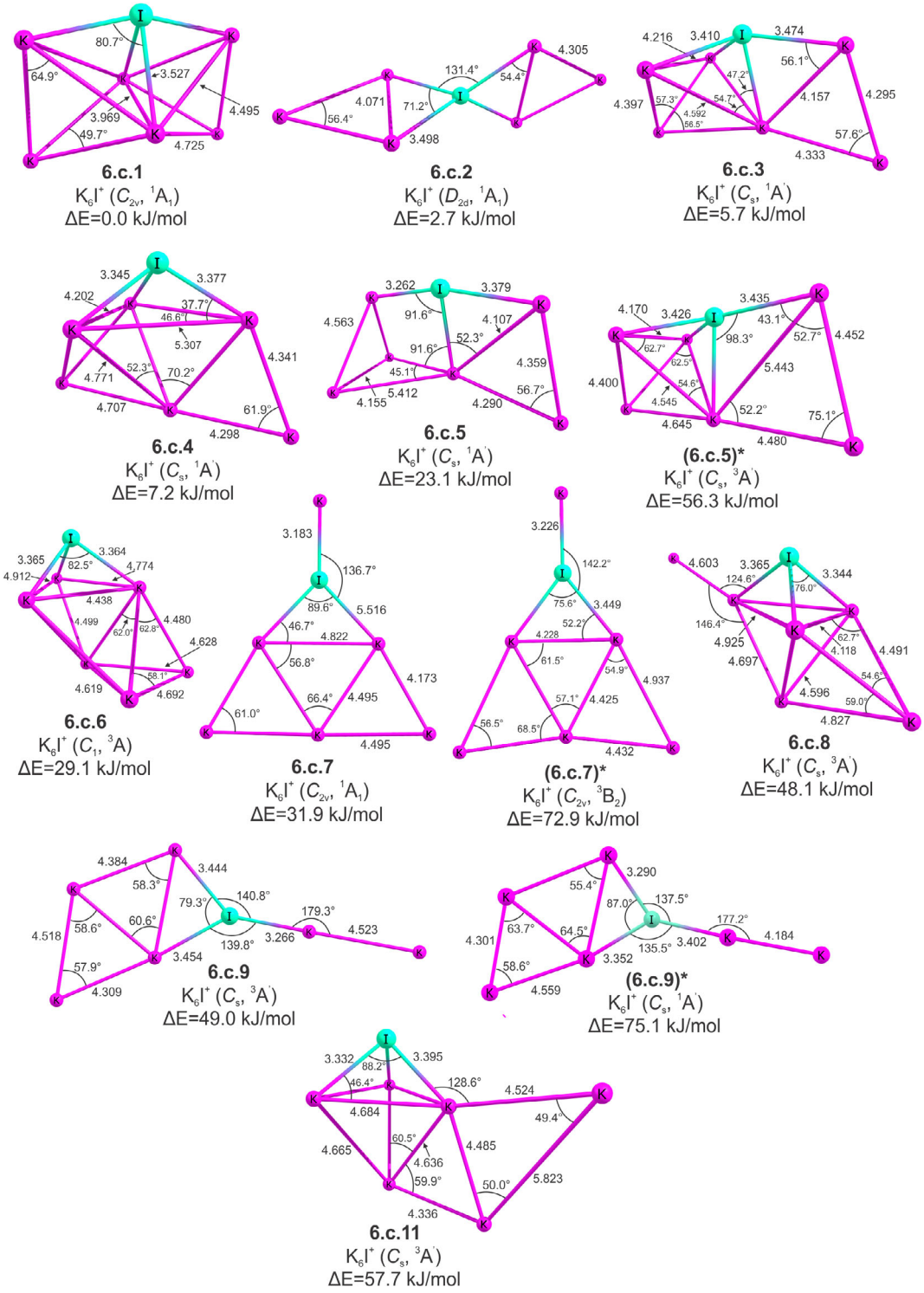

FIGURE 9 Structural isomers of cationic K_nI^+ (n = 6) clusters. The same type computed data as in previous figures

4.4.2 | Dissociation energies

Dissociation energy (D_e) for reactions of the most stable $K_nI^{0,+1}$ (n = 2–6) clusters in which the product is the neutral K atom or cation K^+, calculated at two levels of theory: B3P86/ECP10MDF(K), cc-pVTZ-PP(I) and RCCSD(T)/QZ//B3P86/TZ, are presented in Table 2. For most stable $K_nI^{0,+1}$ (n = 1–3) clusters, the RCCSD(T)/QZ//RCCSD(T)/TZ results are also presented, and again they are equal to the RCCSD(T)/QZ//B3P86/TZ results. For all reactions, D_e has a positive value. Dissociation reactions of cationic species are thermodynamically favored when the product is the neutral K atom, except for ionic species KI^+ and K_2I^+. Alternation of dissociation energies between clusters with even and odd electrons is clearly seen for both neutral and cationic clusters.

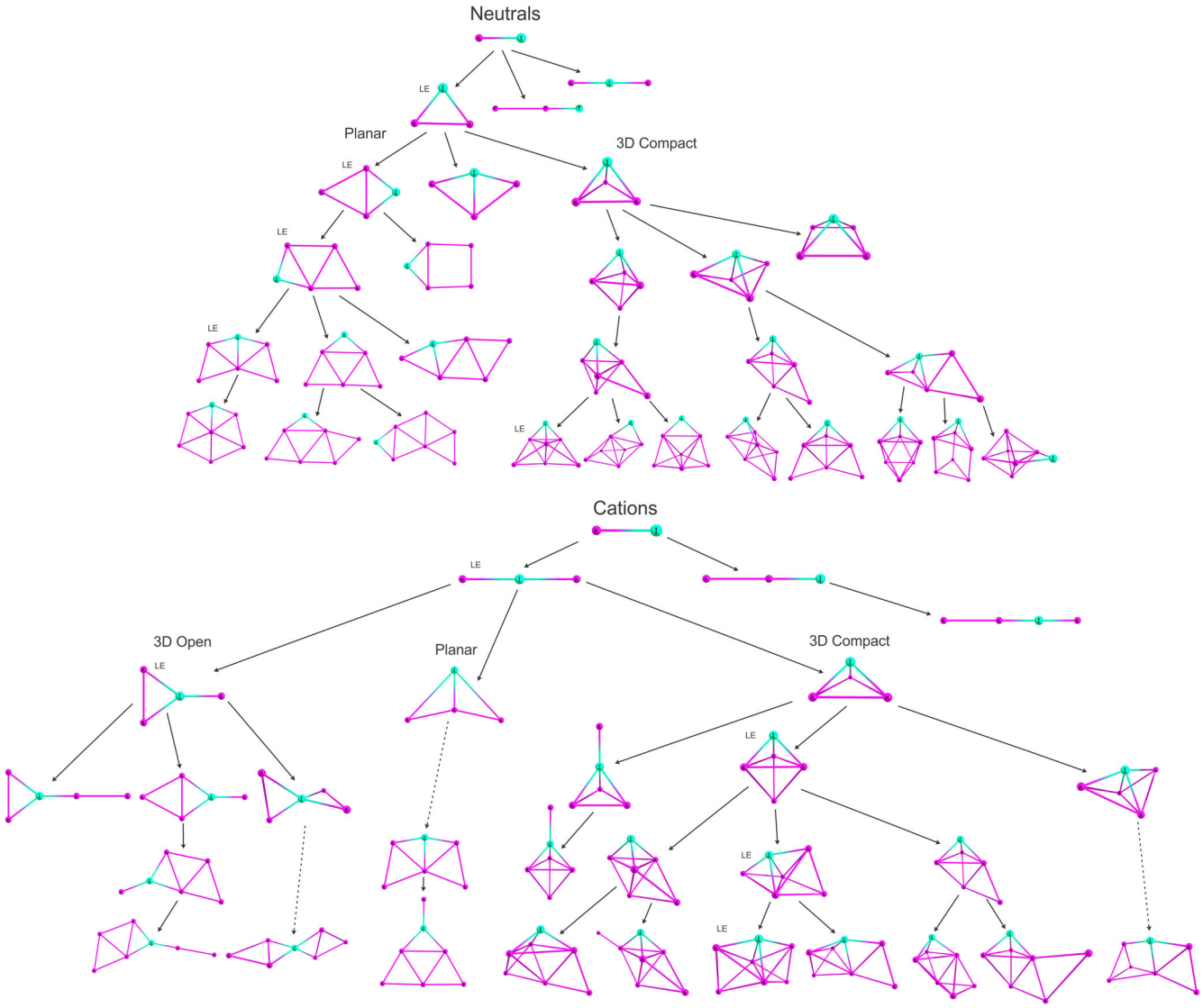

FIGURE 10 Schematic depiction of growth mechanism of $K_nI^{(0,+1)}$ clusters up to the seven atoms

TABLE 1 Binding energy per atom (in eV) for the most stable potassium-iodide clusters

Species $K_nI^{(0,+1)}$	Binding energy per atom
KI	1.77[a] 1.78[b] 1.78[b]
K_2I	1.40[a] 1.43[b] 1.43[b]
K_3I	1.24[a] 1.29[c] 1.29[b]
K_4I	1.07[a] 1.10[c]
K_5I	1.01[a] 1.07[c]
K_6I	0.93[a] 0.99[c]
KI^+	0.13[a] 0.16[c] 1.16[b]
K_2I^+	1.71[a] 1.75[b] 1.75[b]
K_3I^+	1.40[a] 1.43[c] 1.43[b]
K_4I^+	1.29[a] 1.35[c]
K_5I^+	1.16[a] 1.20[c]
K_6I^+	1.11[a] 1.17[c]

[a]B3P86/ECP10MDF(K), cc-pVTZ-PP(I).
[b]RCCSD(T)/QZ//RCCSD(T)/TZ.
[c]RCCSD(T)/QZ//B3P86/TZ.

Theoretical results for dissociation energies are in good agreement with experimentally observed stabilities: K_2I^+ has the highest peak's intensity and the highest D_e, the following are K_4I^+ and K_6I^+ with D_e of 1.03 eV and 0.97 eV, respectively. The lowest calculated D_e possesses K_3I^+ (0.47 eV), and D_e for K_5I^+ is very close to it (0.49 eV). Therefore, theoretically obtained predictions for dissociation energies could qualitatively indicate the cluster stability in our experimental setup—the only deviation is too low value of D_e for K_3I^+.

4.4.3 | Ionization energies

The adiabatic ionization energy (AIE) is computed as the difference in E_{el} + *ZPVE* of a pair of the relaxed cationic and the neutral lowest-energy isomers. The vertical ionization energy (VIE) is calculated as the total energy difference between the electronic energy of the cation having the same geometry as the neutral and the neutral cluster (E_{el} + *ZPVE*). Experimental values together with the adiabatic (AIE) and vertical (VIE) ionization energies for the most stable K_nI (n = 1–6) species, obtained at the B3P86/ECP10MDF(K), cc-pVTZ-PP(I) and RCCSD(T)/QZ//B3P86/TZ level, are outlined in Table 3. Adiabatic (AIE) ionization energies for the most stable K_nI (n = 1–3) species calculated at RCCSD(T)/QZ//RCCSD(T)/TZ level are also presented in Table 3. One can see that DFT values is higher up to 0.7 eV than RCCSD(T) values. Single point RCCSD(T)/QZ values are the same for DFT and coupled cluster geometries.

In literature, three different values of experimental AIE of KI can be found: the first one is 8.2 ± 0.3 eV,[55] obtained by electron impact technique, the second is 7.2 ± 0.1 eV[56] from photoelectron spectroscopy, and the last one is 7.5 ± 0.4 eV,[57] obtained by electron impact technique. Our best result of 7.57 eV (single point RCCSD[T]) agrees with the last one, and is in reasonable agreement with the second one. For experimental VIE of KI there are two values, both obtained from a photoelectron spectrum: 7.4 eV[58] and 7.7 ± 0.1.[56] Our theoretical prediction of 7.75 eV (single point RCCSD[T]) agrees very well with the second one. The first experimental ionization energy of K_2I, obtained by the triple surface ionization, was 3.92 ± 0.1 eV.[28] Our present experimental result (3.98 ± 0.20 eV) is in accord with this value.

From Table 3, it can be seen that experimental values for ionization energies of K_nI (n = 2–6) clusters are in the range of 3.46–3.98 eV. Thus, as all clusters have lower ionization energy than potassium atom (4.34 eV), they could be regarded as "superalkali" clusters.

There are significant structural rearrangements upon formation of the cations, and as a result the difference between the adiabatic and vertical IEs is prominent. However, the adiabatic (vertical) IEs should be a lower (upper) bond to experimentally determined IEs. If one compares theoretically

TABLE 2 Dissociation energy (in eV) for the most stable potassium-iodide clusters

Reaction	D_e
$K_nI = K_{n-1}I + K$	
$KI = I + K$	3.53[a] 3.56[b] 3.56[c]
$K_2I = KI + K$	0.67[a] 0.73[b] 0.73[c]
$K_3I = K_2I + K$	0.76[a] 0.88[b] 0.88[c]
$K_4I = K_3I + K$	0.37[a] 0.33[b]
$K_5I = K_4I + K$	0.70[a] 0.91[b]
$K_6I = K_5I + K$	0.49[a] 0.50[b]
$K_nI^+ = K_{n-1}I^+ + K$	
$KI^+ = I^+ + K$	6.58[a] 6.50[b] 6.50[c]
$K_2I^+ = KI^+ + K$	4.87[a] 4.92[b] 4.92[c]
$K_3I^+ = K_2I^+ + K$	0.46[a] 0.47[b] 0.47[c]
$K_4I^+ = K_3I^+ + K$	0.88[a] 1.03[b]
$K_5I^+ = K_4I^+ + K$	0.52[a] 0.49[b]
$K_6I^+ = K_5I^+ + K$	0.76[a] 0.97[b]
$K_nI^+ = K_{n-1}I + K^+$	
$KI^+ = I + K^+$	0.26[a] 0.32[b] 0.32[c]
$K_2I^+ = KI + K^+$	1.59[a] 1.68[b] 1.68[c]
$K_3I^+ = K_2I + K^+$	1.38[a] 1.42[b] 1.42[c]
$K_4I^+ = K_3I + K^+$	1.50[a] 1.56[b]
$K_5I^+ = K_4I + K^+$	1.64[a] 1.72[b]
$K_6I^+ = K_5I + K^+$	1.71[a] 1.78[b]

[a]B3P86/ECP10MDF(K), cc-pVTZ-PP(I).
[b]RCCSD(T)/QZ//B3P86/TZ.
[c]RCCSD(T)/QZ//RCCSD(T)/TZ.

TABLE 3 Experimental and computed adiabatic, vertical ionization energies (in eV) for potassium-iodide clusters

	AIE		VIE		
K_nI	Transition	Value	Transition	Value	Exp
KI	**1.n.1** → **1.c.1**	8.17[a] 7.57[b] 7.57[c]	**1.n.1** $^1\sum^+ \rightarrow {}^2\prod$	8.31[a] 7.75[b]	8.2 ± 0.3[d] 7.2 ± 0.1[e] 7.5 ± 0.4[f] 7.4[g] 7.7 ± 0.1[h]
K_2I	**2.n.1** → **2.c.1**	3.98[a] 3.39[b] 3.39[c]	**2.n.1** $^2A_1 \rightarrow {}^1A_1$	4.61[a] 4.09[b]	3.92 ± 0.10[i] 3.98 ± 0.20[j]
K_3I	**3.n.1** → **3.c.1**	4.28[a] 3.80[b] 3.80[c]	**3.n.1** $^1A_1 \rightarrow {}^2A_1$	4.72[a] 4.32[b]	3.74 ± 0.20[j]
K_4I	**4.n.1** → **4.c.1**	3.77[a] 3.10[b]	**4.n.1** $^2A' \rightarrow {}^1A'$	4.28[a] 3.72[b]	3.50 ± 0.20[j]
K_5I	**5.n.1** → **5.c.1**	3.95[a] 3.52[b]	**5.n.1** $^1A_1 \rightarrow {}^2B_1$	4.11[a] 3.84[b]	3.46 ± 0.20[j]
K_6I	**6.n.1** → **6.c.1**	3.68[a] 3.05[b]	**6.n.1** $^2A' \rightarrow {}^1A'$	3.86[a] 3.32[b]	3.73 ± 0.20[j]

Abbreviations: AIE, adiabatic ionization energy; VIE, vertical ionization energy.
[a]B3P86/ECP10MDF(K), cc-pVTZ-PP(I).
[b]RCCSD(T)/QZ//B3P86/TZ.
[c]RCCSD(T)/QZ//RCCSD(T)/TZ.
[d]Electron impact technique.[55]
[e]Photoelectron spectroscopy.[56]
[f]Electron impact technique.[57]
[g]VIE from photoelectron spectroscopy.[58]
[h]VIE value from photoelectron spectroscopy.[56]
[i]Veličković et al.[28]
[j]This work.

predicted adiabatic and vertical ionization energies (at more reliable RCCSD(T) level) with experimentally obtained values within error bars, it can be seen that for clusters with the even number of electrons (closed-shell: K_3I and K_5I) adiabatic ionization energies are close to experimental values; on the other hand, for clusters with odd number of electrons (open-shell: K_2I, K_4I, and K_6I), the vertical ionization energies are close to experimental values. This can be rationalized considering definition of adiabatic and vertical ionization energies and stability of clusters: upon ionization of more stable closed-shell neutral clusters, relaxation of cation geometry occurs and measured ionization energies are adiabatic IE; on the contrary, upon ionization of the less stable open-shell neutral clusters, relaxation of cation geometry is not significant and measured ionization energies are close to the vertical IE.

5 | PRESENT CONCLUSIONS

Heterogeneous potassium-iodide clusters $K_nI^{0,+1}$ (n = 2–6) were produced by KCMS modification method in the temperature range of 1250–1750 K, where clusters with more than three potassium atoms were detected for the first time. Inspection of mass spectrum shows that the peaks from K_2I^+ and K_4I^+ are the most intensive; the peaks corresponding to K_3I^+ and K_6I^+ are less intensive; while the peak of K_5I^+ had the lowest intensity. All ionization energies obtained by mass spectrometry are in the range of 3.46–3.98 eV, and by comparing to IE of K atom (4.34 eV), these clusters could be classified as "superalkali."

We have depicted all low-energy constitutional isomers of the neutral and positively charged $K_nI^{0,+1}$ (n = 2–6) species, obtained by using a stochastic method together with quantum chemistry electronic structure methods. It is found that the single point RCCSD(T)/ECP10MDF(K), cc-pVQZ-PP(I) method in combination with B3P86/ECP10MDF(K), cc-pVTZ-PP(I) geometry optimizations and ZPVE corrections is suitable for calculation of the stability parameters (binding, dissociation and ionization energies) of the title clusters. From the inspection of the lowest-energy structures, we can infer that the best description of the growth mechanism of these clusters is the formation of $K_nI^{(0,+1)}$ from $K_{n-1}I^{(0,+1)}$ by adding one potassium atom. Furthermore, we have shown that doping of pure potassium clusters with iodide considerably contributes to its stability. However, there is a general trend of decreasing of BE with cluster growth. In order to obtain more stable larger heterogeneous clusters, more iodine atoms should be added to potassium than one. The closed-shell species (K_3I, K_5I, K_4I^+, and K_6I^+) have slightly increased stability with respect to the open-shell species (K_2I, K_4I, K_6I, K_3I^+, and K_5I^+). The alternation of dissociation energies between closed-shell and open-shell clusters can be also noticed for both neutral and cationic clusters. If we compare theoretical ionization energies with experimental values, it can be

concluded that for closed-shell clusters, the adiabatic ionization energies are close to the experimental values, while in the case of open-shell clusters the vertical ionization energies are more similar to experimental values. At the end, we note that in comparison to the corresponding lithium clusters with iodine, these are generally less stable.

ACKNOWLEDGMENTS

This work was supported by the Ministry of Education, Science, and Technological Development of the Republic of Serbia (under projects ON-172040 and ON-172019). B.M. thanks Marko Mitić for providing insights and technical expertise that greatly assisted B.M. in his understanding of this scientific field.

ORCID

Branislav Milovanović https://orcid.org/0000-0001-7106-9353
Milan Milovanović https://orcid.org/0000-0001-6409-4534
Suzana Veličković https://orcid.org/0000-0001-5605-6749
Filip Veljković https://orcid.org/0000-0002-4471-334X
Stanka Jerosimić https://orcid.org/0000-0001-5873-0477

REFERENCES

[1] S. A. Claridge, A. W. Castleman, S. N. Khanna, C. B. Murray, A. Sen, P. S. Weiss, *ACS Nano* **2009**, *3*, 244.
[2] S. N. Khanna, P. Jena, *Phys. Rev. B* **1995**, *51*, 13705.
[3] A. N. Alexandrova, A. I. Boldyrev, *J. Phys. Chem. A* **2003**, *107*, 554.
[4] A. Boldyrev, L. Wang, *J. Phys. Chem. A* **2001**, *105*, 10759.
[5] P. Garcia-Fernandez, I. B. Bersuker, *Int. J. Quantum Chem.* **2012**, *112*, 3025.
[6] P. V. R. Schleyer, in *New Horizons of Quantum Chemistry* (Eds: P.O. Lowdin, B. Pullman), Springer, Dordrecht **1983**, p. 95.
[7] G. L. Gutsev, *Chem. Phys. Lett.* **1982**, *92*, 262.
[8] G. L. Gutsev, A. I. Boldyrev, *Chem. Phys.* **1981**, *56*, 277.
[9] E. Rehm, A. I. Boldyrev, P. V. R. Schleyer, *Inorg. Chem.* **1992**, *31*, 4834.
[10] D. E. Bergeron, A. W. Castleman, T. Morisato, S. N. Khanna, *Science* **2004**, *304*, 84.
[11] D. E. Bergeron, P. J. Roach, A. W. Castleman, N. O. Jones, S. N. Khanna, *Science* **2005**, *307*, 231.
[12] R. Donoso, C. Cárdenas, P. Fuentealba, *J. Phys. Chem. A* **2014**, *118*, 1077.
[13] E. Florez, P. Fuentealba, *Int. J. Quantum Chem.* **2009**, *109*, 1080.
[14] A. Banerjee, T. K. Ghanty, A. Chakrabarti, *J. Phys. Chem. A* **2008**, *112*, 12303.
[15] S. Abdalla, M. Springborg, Y. Dong, *Surf. Sci.* **2013**, *608*, 255.
[16] A. Aguado, *Comput. Theor. Chem.* **2013**, *1021*, 135.
[17] M. X. Silva, B. R. L. Galvão, J. C. Belchior, *Phys. Chem. Chem. Phys.* **2014**, *16*, 8895.
[18] L. Padilla-Campos, E. Chávez, *J. Mol. Struct. Theochem* **2010**, *958*, 92.
[19] Y. A. Yang, L. A. Bloomfield, C. Jin, L. S. Wang, R. E. Smalley, *J. Chem. Phys.* **1992**, *96*, 2453.
[20] J. Huang, *J. Mol. Struct.* **2001**, *145*, 567.
[21] J. Huang, L. S. Bartell, *J. Phys. Chem. A* **2002**, *106*, 2404.
[22] S. H. Huh, H. S. Jeong, K. Koyasu, K. Miyajima, M. Mitsui, A. Nakajima, *J. Mol. Struct.* **2008**, *886*, 39.
[23] S. H. Huh, G. H. Lee, *J. Korean Phys. Soc.* **2001**, *38*, 107.
[24] T. M. Barlak, J. E. Campana, R. J. Colton, J. J. DeCorpo, J. R. Wyatt, *J. Phys. Chem.* **1981**, *85*, 3840.
[25] G. D. Wang, R. B. Cole, *Anal. Chim. Acta* **2000**, *406*, 53.
[26] J. D. Hogan, D. A. Laude, *J. Am. Soc. Mass Spectrom.* **1992**, *3*, 301.
[27] A. T. Blades, M. Pescahke, U. H. Verkerk, P. Kebarle, *J. Am. Chem. Soc.* **2004**, *126*, 11995.
[28] S. R. Veličković, F. M. Veljković, A. A. Perić-Grujić, B. B. Radak, M. V. Veljković, *Rapid Commun. Mass Spectrom.* **2011**, *25*, 2327.
[29] R. Juraschek, T. Dulcks, M. Karas, *J. Am. Soc. Mass Spectrom.* **1999**, *10*, 300.
[30] H. Kudo, *Nature* **1992**, *355*, 432.
[31] E. F. Fialko, A. V. Kikhtenko, V. B. Goncharov, K. I. Zamaraev, *J. Phys. Chem. A* **1997**, *101*, 8607.
[32] F. M. Veljković, J. B. Djustebek, M. V. Veljković, A. A. Perić-Grujić, S. R. Veličković, *J. Mass Spectrom.* **2012**, *47*, 1495.
[33] M. Saunders, *J. Comput. Chem.* **2004**, *25*, 621.
[34] T. B. Tai, M. T. Nguyen, *J. Chem. Theory Comput.* **2011**, *7*, 1119.
[35] M. Z. Milovanović, S. V. Jerosimić, *Int. J. Quantum Chem.* **2014**, *114*, 192.
[36] M. Milovanović, S. Veličković, F. Veljković, S. Jerosimić, *Phys. Chem. Chem. Phys.* **2017**, *19*, 30481.
[37] A. D. Becke, *J. Chem. Phys.* **1993**, *98*, 5648.
[38] J. P. Perdew, *Phys. Rev. B* **1986**, *33*, 8822.
[39] I. S. Lim, P. Schwerdtfeger, B. Metz, H. Stoll, *J. Chem. Phys.* **2005**, *122*, 104103.
[40] K. A. Peterson, D. Figgen, E. Goll, H. Stoll, M. Dolg, *J. Chem. Phys.* **2003**, *119*, 11113.

[41] K. A. Peterson, T. H. Dunning, *J. Chem. Phys.* **2002**, *117*, 10548.
[42] C. Lee, W. Yang, R. G. Parr, *Phys. Rev. B* **1988**, *37*, 785.
[43] J. P. Perdew, J. A. Chevary, S. H. Vosko, K. A. Jackson, M. R. Pederson, D. J. Singh, C. Fiolhais, *Phys. Rev. B* **1992**, *46*, 6671.
[44] J. Watts, J. Gauss, R. Bartlett, *J. Chem. Phys.* **1993**, *98*, 8718.
[45] P. J. Knowles, C. Hampel, H.-J. Werner, *J. Chem. Phys.* **1993**, *99*, 5219.
[46] P. Knowles, C. Hampel, H. Werner, *J. Chem. Phys.* **2000**, *112*, 3106.
[47] E. Tiemann, H. El Ali, J. Hoeft, T. Torring, *Z. Naturforsch.* **1973**, *28*, 1058.
[48] A. Honig, M. Mandel, M. Stitch, C. Townes, *Phys. Rev.* **1954**, *96*, 629.
[49] M. J. Frisch, G. W. Trucks, H. B. Schlegel, G. E. Scuseria, M. A. Robb, J. R. Cheeseman, G. Scalmani, V. Barone, G. A. Petersson, H. Nakatsuji, X. Li, M. Caricato, A. Marenich, J. Bloino, B. G. Janesko, R. Gomperts, B. Mennucci, H. P. Hratchian, J. V. Ortiz, A. F. Izmaylov, J. L. Sonnenberg, D. Williams-Young, F. Ding, F. Lipparini, F. Egidi, J. Goings, B. Peng, A. Petrone, T. Henderson, D. Ranasinghe, V. G. Zakrzewski, J. Gao, N. Rega, G. Zheng, W. Liang, M. Hada, M. Ehara, K. Toyota, R. Fukuda, J. Hasegawa, M. Ishida, T. Nakajima, Y. Honda, O. Kitao, H. Nakai, T. Vreven, K. Throssell, J. A. Montgomery Jr., J. E. Peralta, F. Ogliaro, M. Bearpark, J. J. Heyd, E. Brothers, K. N. Kudin, V. N. Staroverov, T. Keith, R. Kobayashi, J. Normand, K. Raghavachari, A. Rendell, J. C. Burant, S. S. Iyengar, J. Tomasi, M. Cossi, J. M. Millam, M. Klene, C. Adamo, R. Cammi, J. W. Ochterski, R. L. Martin, K. Morokuma, O. Farkas, J. B. Foresman, D. J. Fox, *Gaussian 09*, *Revision A.02*, Gaussian, Inc., Wallingford, CT **2009**.
[50] X. Li, M. J. Frisch, *J. Chem. Theory Comput.* **2006**, *2*, 835.
[51] G. B. Bacskay, *Chem. Phys.* **1981**, *61*, 385.
[52] H.-J. Werner, P. J. Knowles, G. Knizia, F. R. Manby, M. Schütz, *Wiley Interdiscip. Rev. Comput. Mol. Sci.* **2012**, *2*, 242.
[53] H. J. Werner, P. J. Knowles, G. Knizia, F. R. Manby, M. Schütz, P. Celani, T. Korona, R. Lindh, A. Mitrushenkov, G. Rauhut, K. R. Shamasundar, T. B. Adler, R. D. Amos, A. Bernhardsson, A. Berning, D. L. Cooper, M. J. O. Deegan, A. J. Dobbyn, F. Eckert, E. Goll, C. Hampel, A. Hesselmann, G. Hetzer, T. Hrenar, G. Jansen, C. Köppl, Y. Liu, A. W. Lloyd, R. A. Mata, A. J. May, S. J. McNicholas, W. Meyer, M. E. Mura, A. Nicklass, D. P. O'Neill, P. Palmieri, D. Peng, K. Pflüger, R. Pitzer, M. Reiher, T. Shiozaki, H. Stoll, A. J. Stone, R. Tarroni, T. Thorsteinsson and M. Wang, MOLPRO, version 2012.1, a package of ab initio programs. Available at: http://www.molpro.net.
[54] K. A. Gschneidner, in *Solid State Physics - Advances in Research and Applications*, (Eds: F. Seitz, D. Turnbull), Academic Press, New York and London **1964**, p. 275.
[55] G. Platel, *J. Chim. Phys.* **1965**, *62*, 1176.
[56] A. W. Potts, T. A. Williams, W. C. Price, *Proc. R. Soc. A Math. Phys. Eng. Sci.* **1974**, *341*, 147.
[57] H.-H. Emons, W. Horlbeck, D. Kiessling, *Zeitschrift fur Anorg. und Allg. Chemie* **1982**, *488*, 212.
[58] T. D. Goodman, J. D. Allen, L. C. Cusachs, G. K. Schweitzer, *J. Electron Spectros. Relat. Phenom.* **1974**, *3*, 289.

SUPPORTING INFORMATION

Additional supporting information may be found online in the Supporting Information section at the end of this article.

How to cite this article: Milovanović B, Milovanović M, Veličković S, Veljković F, Perić-Grujić A, Jerosimić S. Theoretical and experimental investigation of geometry and stability of small potassium-iodide K_nI (n = 2–6) clusters. *Int J Quantum Chem*. 2019;119: e26009. https://doi.org/10.1002/qua.26009